16th ICAAR LISBOA 2020-2022

16th International Conference on
Alkali-Aggregate Reaction in Concrete
Lisboa | LNEC | Portugal | 31 May - 2 June 2022

http://icaar2020-2022.lnec.pt

Petrographic Characterization of Highly Reactive Sand from Western Texas, USA

April E. Snyder [(1)], Blake Restelli [(2)], Ashish Patel [(3)], Jerry M. Paris [(4)], Eric R. Giannini [(5)], Christopher C. Ferraro [(6)]

(1) RJ Lee Group, Monroeville, USA, ansyder@rjleegroup.com

(2) RJ Lee Group, Monroeville, USA, brestelli@rjleegroup.com

(3) University of Florida, Gainesville, USA, ashish.patel@ufl.edu

(4) University of Florida, Gainesville, USA, jerry.paris@essie.ufl.edu

(5) Portland Cement Association, La Crosse, USA, egiannini@cement.org

(6) University of Florida, Gainesville, USA, ferraro@ce.ufl.edu

Abstract

Over the past two decades, sand from natural deposits near El Paso, in Western Texas, USA, has been frequently used in alkali-silica reactivity (ASR) research in North America. This sand, commonly known as "Jobe," is known to be highly reactive in all standard laboratory tests and has exhibited a low alkali threshold in exposure site tests at The University of Texas at Austin. As such, it has become an important benchmark aggregate for researchers that enables evaluation of mitigation measures and new laboratory test methods. Despite the frequency of use in ASR research, published information on its mineralogy and petrographic characteristics is limited. As production has moved to different sections of the deposit near the original source first sampled for research, verification of the petrographic characteristics is needed by the research community. This paper details the findings of petrographic characterization of the aggregate according to ASTM C295, Standard Guide for Petrographic Examination of Aggregates for Concrete. Results of accelerated laboratory expansion tests are also detailed and compared to earlier literature. The aggregate consists of six distinct lithologies identified in hand sample and contains abundant amorphous silica and potentially reactive microcrystalline quartz. This work confirms that the recently produced sand from this deposit is both similar in mineralogy to, and similarly or more reactive than, the sand from this source first used at UT-Austin.

***Keywords**: ASR, petrography, mineralogy, expansion testing*

1. INTRODUCTION

Fine aggregate from naturally weathered deposits near El Paso, Texas, USA has been used frequently in ASR research in the past two decades. This sand, often referred to as "Jobe," has been sourced from several pits in close proximity to each other. Its first use appears to have been in conjunction with the development of an outdoor exposure site at The University of Texas at Austin [1]. It has since been documented to exhibit both very high and rapid reactivity in all standard laboratory tests and in outdoor exposure. Outdoor exposure testing also indicates that this aggregate has a very low alkali threshold for deleterious ASR [2,3]. These properties have made it a valuable aggregate for researchers in North America engaged in a variety of ASR-related research activities, including development of new test methods [3-6], evaluating preventive measures to mitigate expansion and techniques to treat ASR-affected structures [1, 2, 7-10], and the use of nondestructive testing (NDT) and structural health monitoring (SHM) methods to quantify ASR damage [11-13]. Despite this widespread use in research, its mineralogy and petrographic characteristics have only been described in cursory fashion in the literature similar to its original description in [1], with some quantitative mineralogical information provided by Stacy and Folliard [3]. The primary objective of the work presented in this paper was to develop a more complete petrographic description of the aggregate that improves upon prior limited reports in the literature.

Over the years, ownership of the pits has changed, and production locations shifted as some areas are mined out. Verification of both the reactivity of recently produced sand from this deposit and its

mineralogical characteristics is needed by the research community. This paper presents the first detailed description of this aggregate according to established petrographic methods (ASTM C295 [14]).

A more extensive investigation is being conducted by the authors to examine the response to mitigation with lithium nitrate of selected reactive aggregates including this aggregate under accelerated laboratory test conditions. This work is ongoing and is beyond the scope of this paper. A comparison of the results of expansion tests conducted in this study to results previously reported in the literature also confirms that the material studied is likely very similar to that used in prior research with regards to potential reactivity. This petrographic description may aid researchers in understanding the exceptional reactivity of this aggregate in different testing regimes and its interaction with mitigation measures such as SCMs and lithium salts.

2. MATERIALS AND METHODS

The experimental program included a detailed petrographic characterization of the highly reactive fine aggregate following ASTM C295, [14]. Expansion testing of the aggregate following ASTM C1260 [15] and AASHTO T 380 [16] was also conducted to confirm that its ASR reactivity is within the historically reported values.

2.1 Materials

The reactive fine aggregate used in this study was acquired in March 2018 from Jobe Materials L.P. (El Paso, Texas, USA). Approximately two tons of the aggregate was sampled by the quarry owner following ASTM D75 [17] and received by the University of Florida for this study. The material was reduced according to ASTM C702 [18] using coning and quartering. Sieve analysis was performed according to ASTM C136 [19] until sufficient quantities were produced to create coned and quartered sub-samples of each size fraction for petrographic analysis.

A non-reactive Miami Oolite limestone coarse aggregate from Gainesville, Florida, USA was sieved to meet the coarse aggregate gradation requirements outlined in AASHTO T 380.

An ASTM C150 Type II ordinary portland cement (OPC) with an equivalent alkali (Na_2O_{eq}) content of 0.94% by mass from Lehigh Cement (Nazareth, Pennsylvania, USA plant) was used in the ASTM C1260 and AASHTO T 380 specimens for ASR expansion testing. The chemical oxide profile, loss on ignition (LOI), and the mineralogical composition (Bogue) of the cement from the manufacturer's mill certification report are presented in Table 2.1.

Table 2.1: Elemental oxide and mineralogical composition of the OPC from the manufacture's mill certification report

Chemical Oxide	Weight %
SiO_2	19.1
Al_2O_3	4.38
Fe_2O_3	3.76
CaO	62.3
MgO	2.86
SO_3	3.04
Na_2O	0.33
K_2O	0.92
Na_2O_{eq}	0.94
LOI	2.56
Bogue Mineral Phase	Weight %
C_3S	58.2
C_2S	13.2
C_3A	5.47
C_4AF	11.9

Reagent grade sodium hydroxide pellets were used to produce the 1N NaOH soak solutions in ASTM C1260 and AASHTO T 380 testing and added to the mixing water to boost the alkali content of the AASHTO T 380 specimens to 1.25% by mass of cement.

2.2 Petrographic Examination

The fine aggregate sample was reduced for testing following ASTM C702 [18] and a sample of 329 grams was sieved following ASTM C136 [19]. Each size fraction of the material retained on 9.5 mm (3/8 inch), 4.75 mm (No. 4), 2.38 mm (No. 8), 1.19 mm (No. 16), 0.60 mm (No. 30), 0.300 mm (No. 50), and 0.150 mm (No. 100) sieves, was collected for examination.

Petrographic examination was performed following ASTM C295. Particles retained on each sieve were examined under a binocular microscope at up to 50x magnification and sorted into rock types based on hand specimen lithological characteristics. Sorting was performed by with a specific objective to uncover potential differences in reactive components that could be correlated with expansion test results. The weight percentage of each lithology was determined for 150 particles retained on each sieve from 9.5 mm (3/8 in.) to 0.60 mm (No. 30). The number of particles examined from of these sieve sizes was consistent with ASTM C295. This standard is intended to be one part of evaluating aggregates for use in concrete, with a particular focus on identifying potentially deleterious components that may necessitate further investigation. Further investigation may include, for example, expansion testing of mortar or concrete when potentially reactive constituents are identified. ASTM C295 is not necessarily intended for precise quantification of each mineral or lithology present, given the statistical limitations associated with evaluating this number of particles.

Particles passing the 0.60 mm (No. 30) sieve were primarily comprised of individual mineral grain particles weathered from the different lithologies present in the aggregate and were analyzed using X-ray diffraction (XRD). Quantitative X-ray diffraction (qXRD) analysis with Rietveld refinement was performed on a sample representing all size fractions of the aggregate, a sample of material passing the 0.60 mm (No. 30) sieve and retained on the 0.300 mm (No. 50) sieve, and a sample of material passing the 0.300 mm (No. 50) and retained on the 0.150 mm (No. 100) sieve. Each sample was ground to pass through a 0.075 mm (No. 200) sieve for XRD analyses. Size reduction was performed using a stainless-steel ball mill and isopropanol as an anticoagulant. After size reduction, the powder was evenly packed into a metal holder ring using a glass slide and a razor blade.

Samples were analyzed using a PANalytical X'Pert Pro diffractometer using Cu-Kα radiation from 4 to 75° 2Θ with a step size of 0.008° 2Θ for 240 seconds per step. The resulting diffraction pattern was then analyzed using X'Pert HighScore Plus search-match software utilizing the ICDD PDF4+ database to identify the phases present. HighScore Plus was also utilized to attempt to quantify the phases present in the sample by Rietveld refinement. Rietveld refinement is a full-pattern fitting method, the goal of which is to use structural data from the PDF4+ database to construct a calculated profile that is as similar as possible to the measured profile of the sample, as obtained by XRD. By refining the model, the differences between the two profiles are minimized and each phase can be quantified. Additionally, an external standard (fluorite, CaF_2) was run by XRD under the same parameters as the sample. The standard was modeled, and an external k-factor was calculated by the X'Pert HighScore Plus software. The k-factor was then applied to the Rietveld model of the sample to determine the percentage of amorphous material present. The qXRD analyses yielded the weight percentage of each mineral identified and the determined amorphous material.

Representative aggregate particles were prepared as petrographic thin sections for further examination. Particles were mounted to a glass reference slide with auto body putty and then ground into using a Pelcon thin sectioning machine. Once flat, the slides and their particles were impregnated with Buehler EpoThin 2 epoxy. After curing, the samples were ground into and mounted to an objective slide. A diamond blade was used to cut the mounted aggregate to an approximate thickness of 0.4 mm. Additional grinding was performed using diamond plated rollers on the thin section machine to a thickness of approximately 0.08 mm. Final grinding and polishing were completed by hand on a series of plates and pads with Buehler MetaDi diamond suspension to achieve a thickness of 0.03 mm.

Thin section selection and analysis were conducted for precise rock and mineral identification and to identify potentially ASR reactive constituents and other potentially deleterious components for use in concrete. Polarized-light microscopy at up to 400x magnification was used for examination of the thin sections.

2.3 Reactivity Testing

Expansion tests were conducted on the fine aggregate to compare its reactivity characteristics against prior work reported in the literature. Both ASTM C1260 (accelerated mortar bar test, or AMBT) and AASHTO T 380 (miniature concrete prism test, or MCPT) were performed.

3. RESULTS AND DISCUSSION

3.1 Petrographic Characterization

The natural sand fine aggregate consisted of a variety of rock types and minerals in the smallest sieve fractions. The rock types were primarily igneous with a trace amount of sandstone and chert. A total of six unique lithologies were identified in the fraction of the fine aggregate retained on the 0.60 mm (No. 30) and larger sieves. These were designated L1 through L6. The finer material retained on the 0.300 mm (No. 50) and 0.150 mm (No. 100) sieves, which constituted 60 percent of the total weight of the aggregate, was found to consist of particles of quartz (F1), feldspars (F2), mica/illiite (F3), and amorphous material (F4). Table 3.1 summarizes the overall composition of the fine aggregate larger than 0.150 mm (No. 100 sieve size), as determined by the combined particle count and qXRD analyses. This was determined by weighting the particle counts and mineral quantity on each sieve size by the total fraction of the aggregate retained on each sieve obtained from the sieve analysis. Percentages are rounded to whole numbers consistent with ASTM C295 reporting requirements, and some constituents are grouped (e.g. mica and illite) to ensure the total quantities round up to 100 percent. The reported quantities in Table 3.1 reflect what is present in the single sample of aggregate provided by the quarry and do not necessarily reflect any natural variation that may exist throughout the quarry as it has been mined over time. Detailed descriptions of the lithologies and mineralogical characteristics are presented in section 3.1.1.

Table 3.1: Calculated weight percentage composition of fine aggregate by particle count and qXRD.

Rock Type or Mineral Phase with Approximate Composition	Weight % of Total Aggregate*
L1 – Granite	22
L2 – Mafic/Basalt	1
L3 – Volcanics	11
L4 – Sandstone	1
L5 – Pumice	1
L6 – Chert	2
F1 – Quartz particles (SiO_2)	36
F2 – Feldspar particles (K-feldspar & plagioclase)	15
F3 – Mica/Illite particles	2
F4 – Amorphous particles	10
Total	100

*Standard Rounding rules applied.

The rock types identified in the aggregate contain known highly reactive silica components including microcrystalline quartz in the chert and amorphous silica or glass in the basalt, rhyolite, and pumice. The granite contained a moderate-low reactive strained quartz. The weathering of these rock types leaves behind fine particles of resistant minerals contained in each rock and resulted in an abundance of potentially reactive quartz and amorphous silica in the size fractions smaller than the 0.60 mm (No. 30) sieve.

3.1.1 Rock Type Lithologies

Rock type L1, shown in Figure 3.1 and in thin section in Figure 3.2, consisted of very weathered granite particles containing quartz and feldspar with minor muscovite grains. A moderate amount of strained quartz was observed in this rock type. Particles were multi-colored, with Munsell colors 5YR 7/2 grayish pink, 10YR 6/2 pale yellowish brown, and 5YR 6/1 light brownish gray all present. Particles were rounded to sub-rounded in shape. Mineral grains were euhedral in shape and phaneritic (coarse) in size. Moh's hardness ranged from 6 to 7.

Rock type L2, shown in Figure 3.1 and in thin section in Figure 3.3, consisted of moderately to very weathered basalt particles containing olivine, quartz, plagioclase, pyroxenes, and opaque minerals. Particles were predominantly gray in color (Munsell N3 dark gray and N4 medium dark grey). Particles were sub-rounded to sub-angular in shape. Mineral grains were subhedral in shape and aphanitic (fine-grained) in size. Moh's hardness ranged from 6 to 6.5 and minor porosity was observed in some particles.

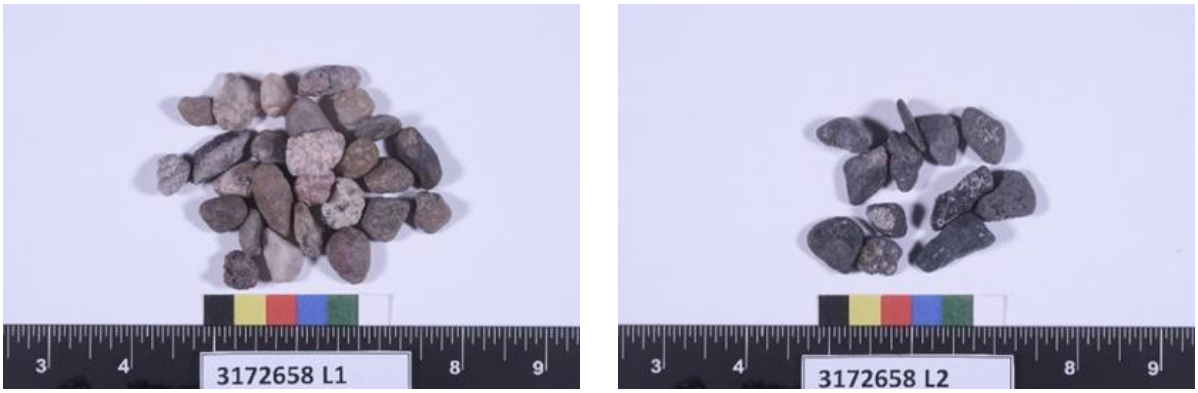

Figure 3.1: Photographs of rock types L1, granite (left) and L2, mafic/basalt (right).

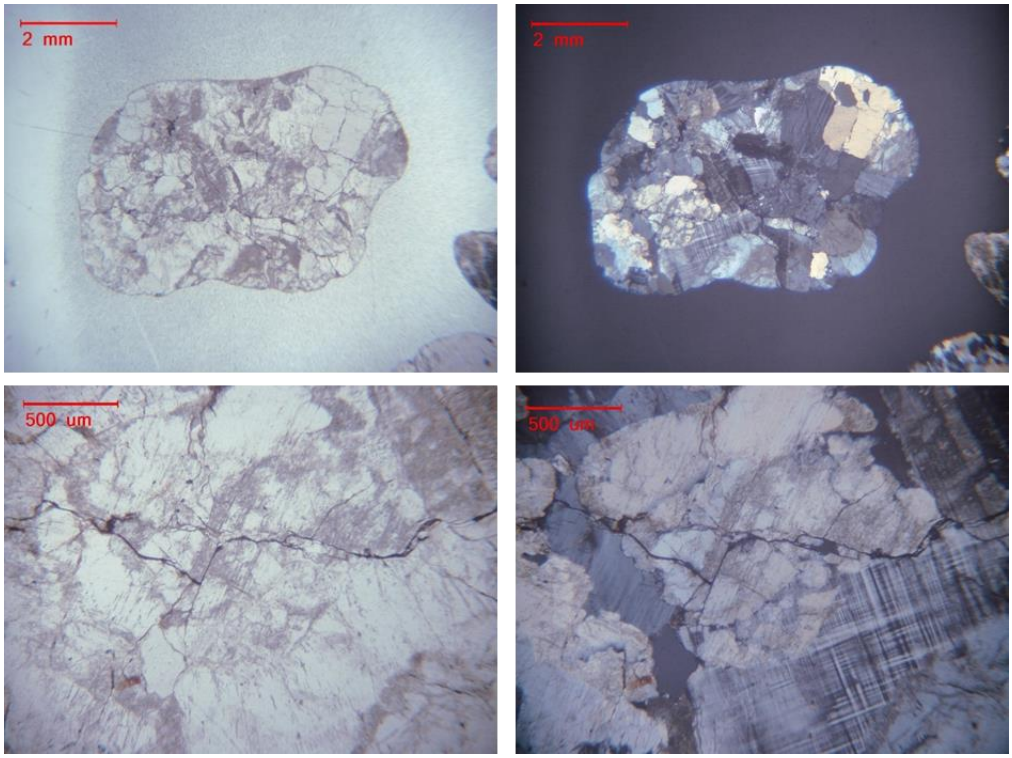

Figure 3.2: Photomicrographs of L1, granite, in PPL (left) and XPL (right).

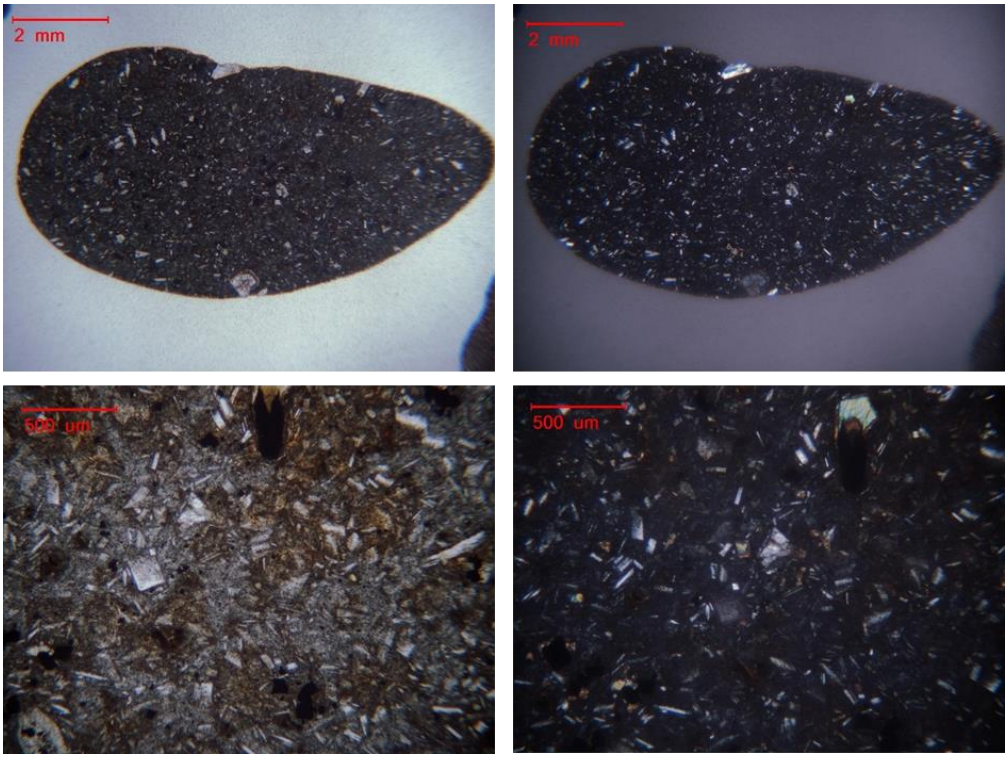

Figure 3.3: Photomicrographs of L2, basalt, in PPL (left) and XPL (right).

Rock type L3, shown in Figure 3.4 and in thin section in Figure 3.5, consisted of very weathered volcanic particles (a mix of rhyolite, dacite, andesite) containing large phenocrysts of plagioclase and monocrystalline quartz in a very fine siliceous groundmass containing cryptocrystalline quartz and glass. Particles were multi-colored, with Munsell colors 10YR 8/2 grayish orange pink, N6 medium light gray, and 5Y 6/1 light olive gray all present. Particles were sub-rounded to sub-angular in shape. Mineral grains were subhedral in shape with a porphyritic texture. Major alterations and areas of recrystallization were observed along with major staining and altered coloration. Moh's hardness ranged from 6 to 7.

Rock type L4, shown in Figure 3.4, consisted of porous and very weathered sandstone particles containing quartz (including strained and microcrystalline), feldspars, micas, and opaque minerals. Particles were multi-colored, with Munsell colors 5YR 7/2 grayish pink, 10YR 6/2 pale yellowish brown, and 5YR 6/1 light brownish gray all present. Particles were sub-rounded to sub-angular in shape. Grains were very coarse to medium in size and poorly sorted. Moh's hardness ranged from 6 to 7, but due to the friable nature of this rock type, there was an overall lower hardness.

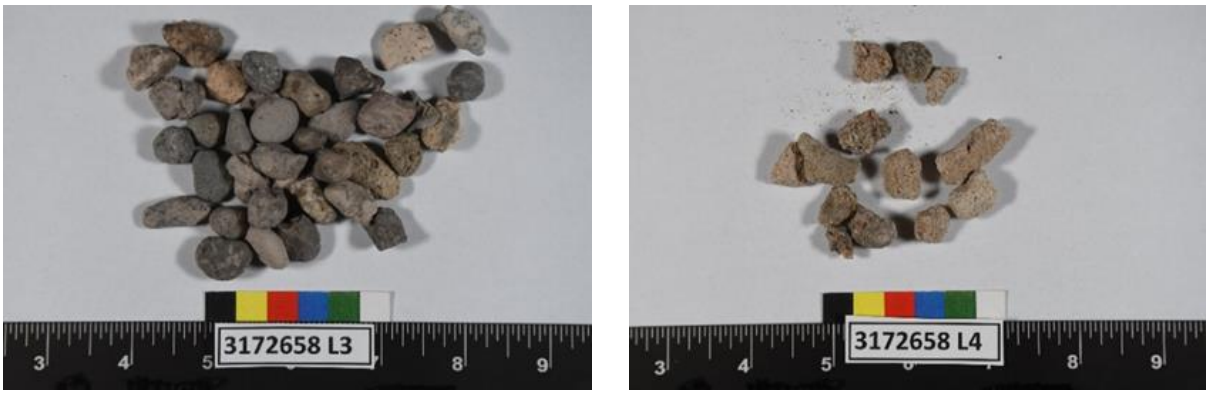

Figure 3.4: Photographs of rock types L3, volcanics (left) and L4, sandstone (right).

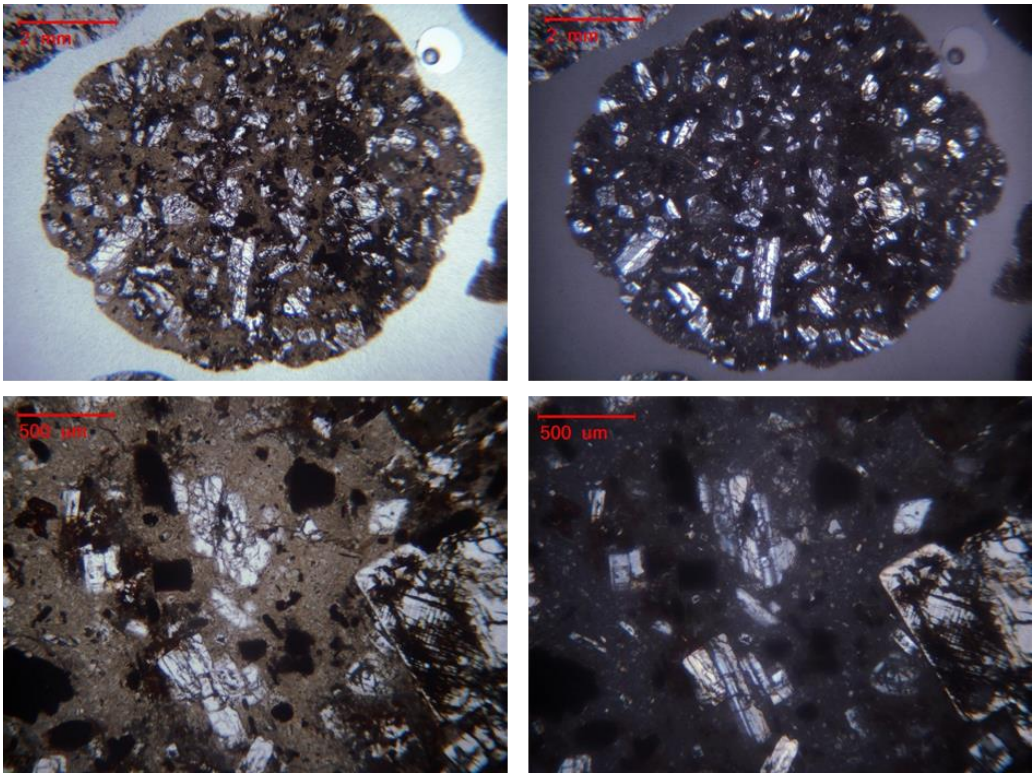

Figure 3.5: Photomicrographs of L3, andesite, in PPL (left) and XPL (right).

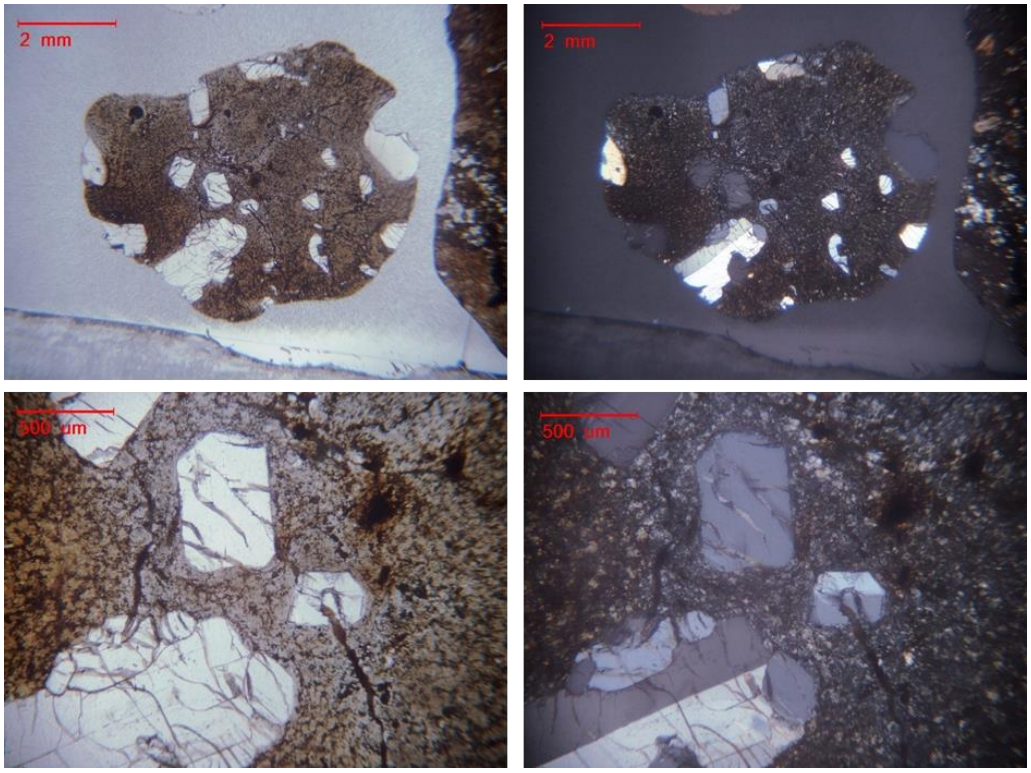

Figure 3.6: Photomicrographs of L3, rhyolite, in PPL (left) and XPL (right).

Rock type L5, shown in Figure 3.7, consisted of very weathered pumice particles containing feldspars, hornblende, and augite, with moderate pyroclasts. Pyroclasts, in this case, are fragments of the surrounding sedimentary and/or metamorphic country rock. Particles were Munsell 5YR 8/1 pinkish gray

in color and sub-angular to angular in shape. Grains were very fine (aphanitic) in size. Particles were vesicular and friable with Moh's hardness ranging from 5 to 6.

Rock type L6, shown in Figure 3.7 and in thin section in 3.8, consisted of very weathered chert and flint particles containing predominantly cryptocrystalline quartz and highly strained quartz grains. Particles were multi-colored, with Munsell colors 5R 3/4 dusky red, 5YR 5/2 pale brown, and N9 white all present. Particles were rounded to sub-rounded in shape, non-clastic, and very fine with a vitreous (glassy) texture. Bands of recrystallized quartz were also observed. Moh's hardness was 7.

Figure 3.7: Photographs of rock types L5, pumice (left) and L6, chert (right).

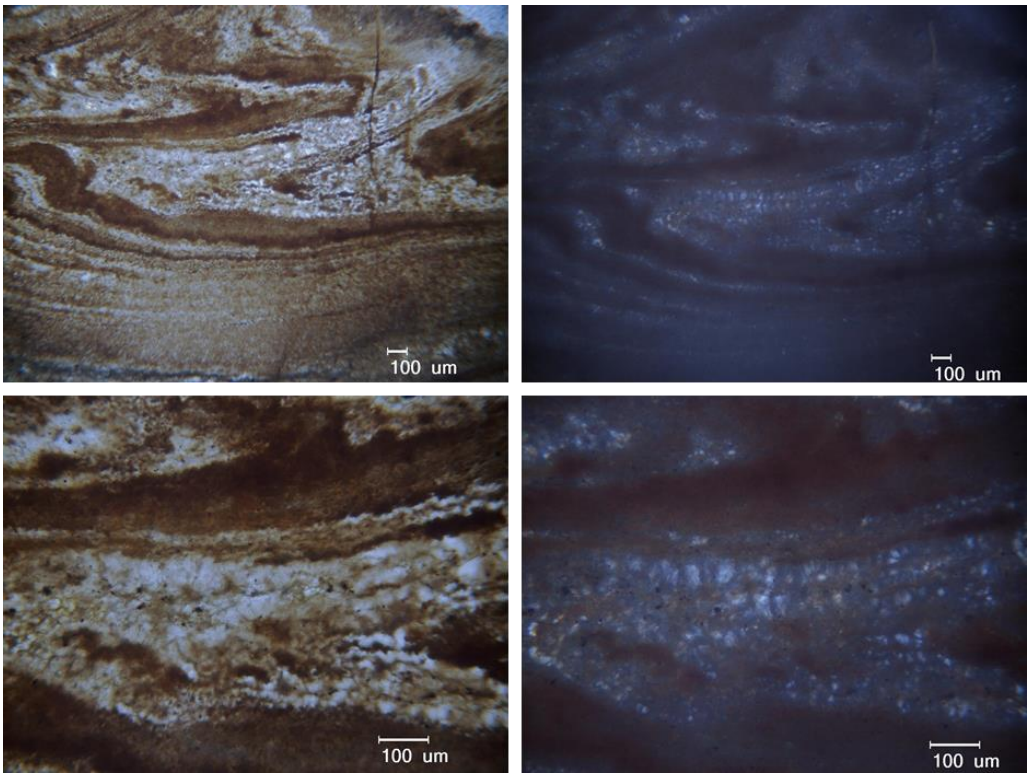

Figure 3.8: Photomicrographs of L6, chert, in PPL (left) and XPL (right).

3.1.2 XRD Analyses

The results of the XRD analyses are summarized in Table 3.2, which presents the quantified percentage of each mineral, along with the percentage amorphous material, identified in the total aggregate, as well as in each of the two fine size fractions. Figures 3.9 through 3.11 present the diffraction patterns for the ungraded and graded samples that were analyzed. Quartz and feldspars constituted the majority of the aggregate and the two fine size fractions, but substantial quantities of amorphous material were identified. Approximately 10 percent of the total aggregate was identified as amorphous, including 18 percent of the material passing the 0.60 mm (No. 30) sieve and retained on the 0.30 mm (No. 50) sieve.

The amorphous minerals were presumably made up of volcanic glass based on the petrography of the coarser size fractions, with some potential for opal from chert and flint.

Table 3.2: XRD quantification by Rietveld Method. All values are weight %.

Phase	Ungraded Aggregate	Passing 0.60 mm (No. 30) and retained on 0.30 mm (No. 50)	Passing 0.30 mm (No. 50) and retained on 0.15 mm (No. 100)
Quartz	56	57	59
Plagioclase Feldspar (s)	20	13	17
K-Feldspar	12	10	10
Mica/Illite	2	3	2
Amorphous	10	18	12

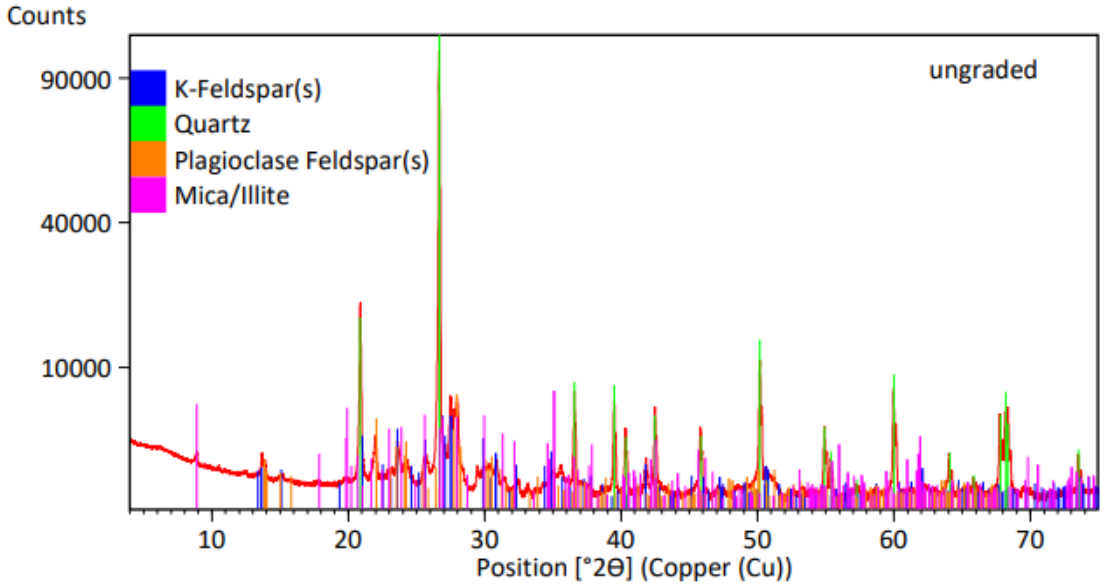

Figure 3.9: XRD pattern for ungraded aggregate.

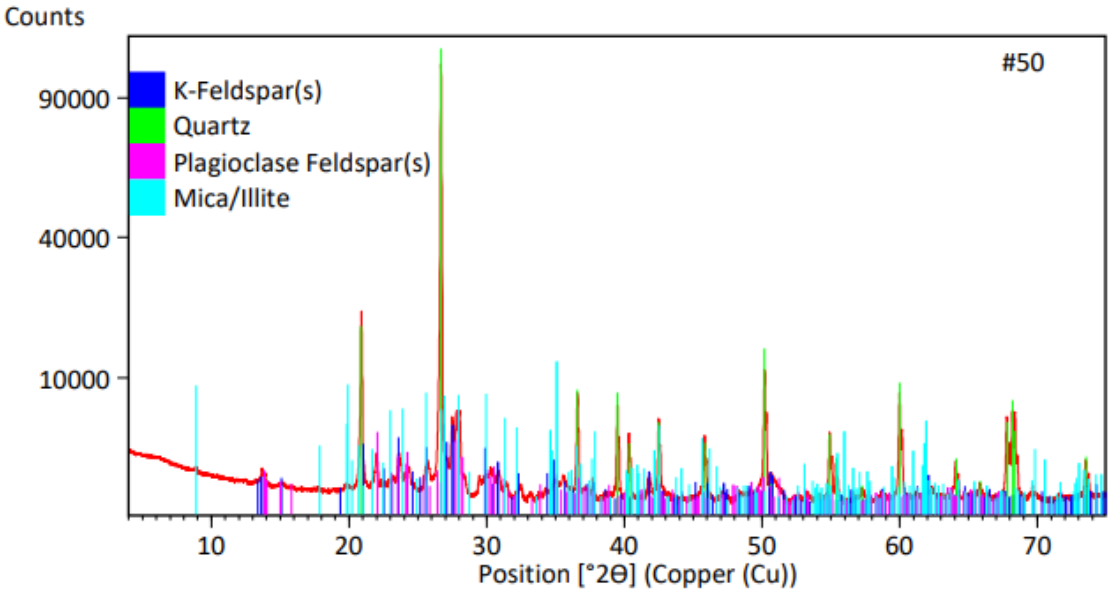

Figure 3.10: XRD pattern for aggregate passing 0.60 mm (No. 30) sieve and retained on 0.30 mm (No. 50) sieve.

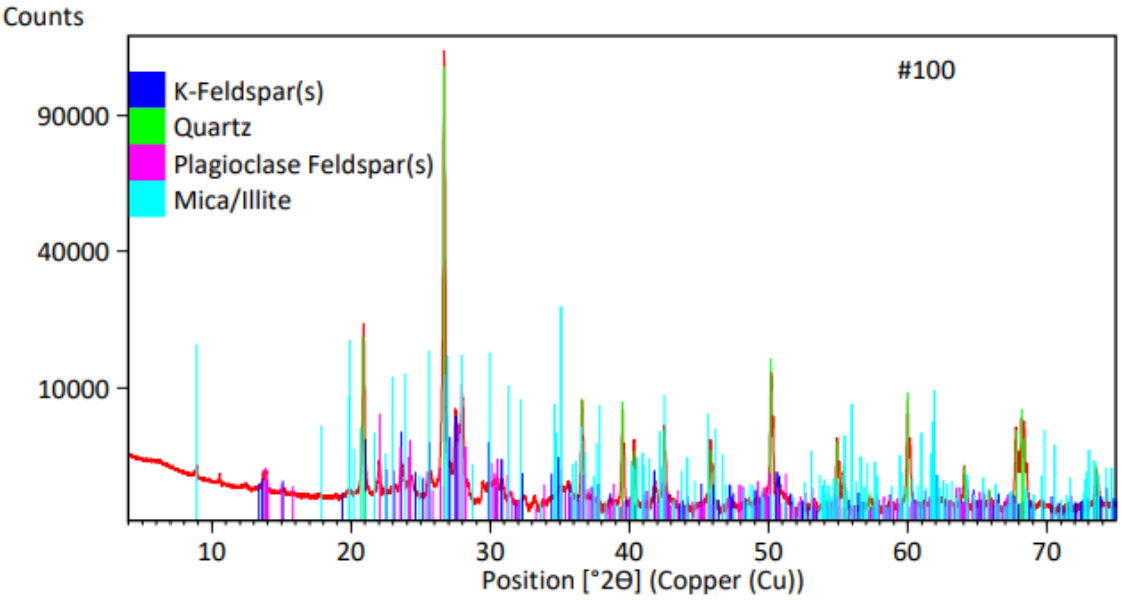

Figure 3.11: XRD pattern for aggregate passing 0.30 mm (No. 50) sieve and retained on 0.15 mm (No. 100) sieve.

3.2 Reactivity Testing

The average 14-day expansion in ASTM C1260 testing was 0.59%. Prior 14-day expansion results reported in the literature for fine aggregate at this and nearby quarries were 0.64% [1], 0.82% [7], and 0.47% [9]. In AASHTO T 380 testing, the average 56-day expansion was 0.457%. Prior 56-day expansion results reported in the literature were 0.440% and 0.435% [4] and 0.643% [10].

The ASTM C1260 expansion results for the aggregate sample used in this work would yield a reactivity classification of very highly reactive (R3) according to ASTM C1778 [20]. The aggregate source would generally be classified at this reactivity level based upon the prior test results in the literature. This suggests the material examined petrographically is substantially similar to that which has been previously used for ASR testing in prior studies.

4. CONCLUSIONS

A highly reactive fine aggregate from El Paso, Texas, USA, commonly referred to as “Jobe” was characterized petrographically following ASTM C295. The petrographic examination included hand sorting, optical microscopy of thin sections under plane-polarized and cross-polarized light, and quantitative XRD using Rietveld refinement. The findings can be summarized as follows:

- The coarser fraction of the fine aggregate, larger than a 0.60 mm (No. 30) sieve, was found to consist of six distinct lithologies. Granite and volcanics (rhyolite and andesite) were the predominant lithologies in this coarser size fraction of the aggregate, while smaller amounts of basalt, sandstone, pumice, and chert were also identified.

- Potentially alkali-silica reactive components identified in the coarser fraction included volcanic glass, microcrystalline quartz, cryptocrystalline quartz, and strained quartz. These were present in rock types commonly known to be deleteriously reactive including rhyolite, andesite, chert.

- The finer fractions of the aggregate, smaller than a 0.60 mm (No. 30) sieve, were characterized by XRD and found to consist predominantly of quartz, feldspars, and amorphous material, along with minor quantities of mica and illite.

- Reactivity in the fine fraction is likely to be primarily caused by the substantial quantity of amorphous material, in addition to probable microcrystalline and strained quartz particles in the crystalline quartz population.

- Expansion testing of the aggregate according to ASTM C1260 (AMBT) and AASHTO T 380 (MCPT) confirms both the highly reactive nature of this particular fine aggregate sample and that its reactivity is similar to that reported in the literature by other researchers using material from this or adjacent locations.

- The variability exhibited in expansion test results may be partly due to inherent variability of the test methods, but also due to variability in the aggregate source deposit. Researchers obtaining samples from this source in the future may improve the understanding of its variability by conducting petrographic examination following ASTM C295 on those samples.

5. REFERENCES

[1] Folliard KJ, Barborak R, Drimalas T, Du L, Garber S, Ideker J, Ley T, Williams S, Juenger M, Fournier B, Thomas MDA (2006) Preventing ASR/DEF in New Concrete: Final Report, FHWA/TX-06/0-4085-5.

[2] Thomas MDA, Fournier B, Folliard KJ (2012) Selecting Measures to Prevent Deleterious Alkali-Silica Reaction in Concrete: Rationale for the AASHTO PP65 Prescriptive Approach, FHWA-HIF-13-002.

[3] Stacy S, Folliard K, Drimalas T, Thomas MDA (2016) An Accelerated and More Accurate Test Method to ASTM C1293: The Concrete Cylinder Test, Proc. 15th ICAAR, Paper No. 130, Sao Paulo.

[4] Latifee E (2013) Miniature Concrete Prism Test - a New Test Method for Evaluating the ASR Potential of Aggregates, the Effectiveness of ASR Mitigation and the Job Mixture. Dissertation, Clemson University.

[5] Wood SG, Giannini ER, Bentivegna AF, Rashidian-Dezfouli H, Rangaraju PR, Drimalas T, Ramsey MA, Johnson TR, Moser RD (2017) Five-Hour Autoclave Test for Determining Potential Alkali-Silica Reactivity of Concrete Aggregates: A Multi-Laboratory Study, Advances in Civil Engineering Materials 6(1): 550-563. https://doi.org/10.1520/ACEM20170061

[6] Giannini ER, Folliard KJ (2013) Determining Alkali-Silica Reactivity of Aggregates Using a Rapid Autoclaved Concrete Prism Test, R&D Serial No. SN3235, Portland Cement Association.

[7] Giannini ER, Bentivegna AB, Folliard KJ (2014) Strain Gradients in Concrete Affected by Alkali-Silica Reaction: A Laboratory Simulation, Advances in Civil Engineering Materials 3:388-403. https://doi.org/10.1520/ACEM20130114

[8] Ideker JH, Bentivegna AB, Folliard KJ, Juenger MG (2012) Do Current Laboratory Test Methods Accurately Predict Alkali-Silica Reactivity? ACI Materials Journal 109:395-402.

[9] Philips WJ, Deschenes R, Hale W (2015) Alkali Silica Reaction Mitigation Using High Volume Class C Fly Ash, World of Coal Ash (WOCA) Conference, Nashville.

[10] Chopperla KST, Drimalas T, Beyene M, Tanesa J, Folliard K, Ardani A, Ideker JH (2022) Combining reliable performance testing and binder properties to determine preventive measures for alkali-silica reaction. Cement and Concrete Research 151:106641. https://doi.org/10.1016/j.cemconres.2021.106641

[11] Kim G, Giannini ER, Klenke ND, Kim JY, Kurtis KE, Jacobs LJ (2017) Measuring Alkali-Silica Reaction (ASR) Microscale Damage in Large-Scale Concrete Slabs Using Nonlinear Rayleigh Surface Waves, Journal of Nondestructive Evaluation 36(2):29. https://doi.org/10.1007/s10921-017-0410-z

[12] Kreitman KL, Giannini ER, Webb ZD, Folliard KJ, Zhu, J, Bayrak O (2012) Nondestructive Evaluation of Reinforced Concrete Structures Affected by ASR, Proc. 14th ICAAR, Austin.

[13] Farnam Y, Geiker MR, Bentz D, Weiss J (2015) Acoustic Emission Waveform Characterization of Crack Origin and Mode in Fractured and ASR Damaged Concrete, Cement and Concrete Composites 60:135-145. https://doi.org/10.1016/j.cemconcomp.2015.04.008

[14] ASTM C295/C295M-19 (2019) Standard Guide for Petrographic Examination of Aggregates for Concrete. ASTM International, West Conshohocken. https://doi.org/10.1520/C0295_C0295M-19

[15] ASTM C1260-14 (2014) Standard Test Method for Potential Alkali Reactivity of Aggregates (Mortar-Bar Method). ASTM International, West Conshohocken. https://doi.org/10.1520/C1260-14

[16] AASHTO T 380-19 (2019) Standard Method of Test for Potential Alkali Reactivity of Aggregates and Effectiveness of ASR Mitigation Measures (Miniature Concrete Prism Test, MCPT). AASHTO, Washington.

[17] ASTM D75/D75M-19 (2019) Standard Practice for Sampling Aggregates, ASTM International. West Conshohocken. https://doi.org/10.1520/D0075_D0075M-19

[18] ASTM C702/C702M-18 (2018) Standard Practice for Reducing Samples of Aggregate to Testing Size. ASTM International, West Conshohocken. https://doi.org/10.1520/C0702_C0702M-18

[19] ASTM C136/C136M-19 (2019) Standard Test Method for Sieve Analysis of Fine and Coarse Aggregate. ASTM International, West Conshohocken. https://doi.org/10.1520/C0136_C0136M-19

[20] ASTM C1778-19a (2019) Standard Guide for Reducing the Risk of Deleterious Alkali-Aggregate Reaction in Concrete. ASTM International, West Conshohocken. https://doi.org/10.1520/C1778-19A